Available online at www.sciencedirect.com
ScienceDirect
Mendeleev Commun., 2023, **33**, 525–527

Mendeleev Communications

Influence of xenon difluoride on the optical properties of fluorozirconate and fluorohafnate glasses

Maria N. Brekhovskikh,[*a] **Sergey Kh. Batygov,**[b] **Liudmila V. Moiseeva,**[b] **Liudmila I. Demina,**[c] **Valeria V. Vinokurova**[a] **and Leonid A. Vaimugin**[a]

[a] *N. S. Kurnakov Institute of General and Inorganic Chemistry, Russian Academy of Sciences, 119991 Moscow, Russian Federation. E-mail: mbrekh@igic.ras.ru*
[b] *Prokhorov General Physics Institute, Russian Academy of Sciences, 119991 Moscow, Russian Federation*
[c] *A. N. Frumkin Institute of Physical Chemistry and Electrochemistry, Russian Academy of Sciences, 119991 Moscow, Russian Federation*

DOI: 10.1016/j.mencom.2023.06.027

To study the effect of xenon difluoride as a fluorinating agent on optical properties of glasses in ZBLAN (ZrF_4–BaF_2–LaF_3–AlF_3–NaF) and HBLAN (HfF_4–BaF_2–LaF_3–AlF_3–NaF) systems, their optical transmission in the range from UV to IR was investigated. The treatment of the initial fluorides with XeF_2 was shown to lead to a broadening of the transmission region of the obtained glasses both in the UV and IR ranges. Moreover, the treatment of the batch with xenon difluoride leads to the removal of oxygen-containing impurities that absorb in the region of 2.8 μm.

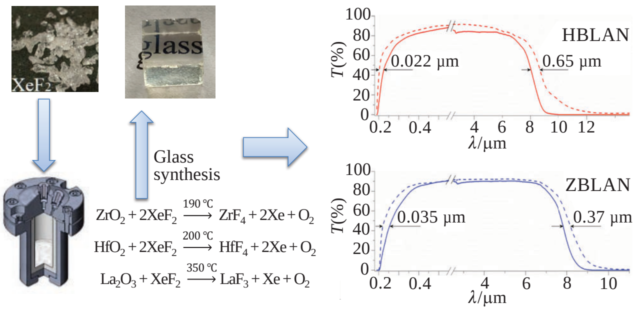

Keywords: fluorozirconate glasses, fluorohafnate glasses, fluoroxidizer, XeF_2, OH^- group, optical transmission.

Fluoride glasses have unique properties and applications. An important advantage of these glasses over quartz glasses is that they are continuously transparent from the near-UV to the mid-IR range (0.295–7.5 μm).[1,2] Their phonon energy is small compared to that of oxide glasses, and they are attractive hosts for rare earth (RE) activators.[3] The formation of phase inhomogeneities due to oxide or oxyfluoride impurities in the initial fluorides leads to a decrease in the fluoride glass transmission. Oxygen-containing impurities also degrade the luminescent characteristics of RE ion activators.[4] First, oxygen absorption bands can overlap with the emission bands of the RE activators; second, high-frequency phonons can be associated with oxygen to increase the rate of nonradiative transitions in activator ions, which leads to a deterioration in the luminescent and laser characteristics of the active media, especially, in the IR region. Therefore, the removal of oxygen-containing impurities from fluoride materials will make it possible to obtain highly efficient luminescent materials emitting in the UV, visible, and mid-IR ranges. In particular, the concentration of OH^- groups in RE, zirconium, and hafnium fluorides and other components of fluoride glasses can be decreased by low-temperature treatment (to 400 °C) of starting materials with ammonium bifluoride to remove adsorbed and chemisorbed water and to fluorinate metal oxide impurities.[5–7] To reduce the oxide and hydroxide content of fluoride materials, the glass batch and the glass melt are exposed to an atmosphere of non-metal fluorides (BF_3, HF, CF_2Cl_2, $CFCl_3$, CF_4, and C_2F_4) in order to replace oxygen by fluorine.[8] However, the efficiency of substitution reactions is insufficient for obtaining oxygen-free materials. Therefore, attempts have been made to use more reactive fluorine-containing reagents, for example, volatile inorganic fluoroxidizers (chlorine and bromine fluorides) in the preparation of materials without absorption bands due to OH^- groups in the IR range.[9,10]

In this work we studied the influence of batch treatment with xenon difluoride on optical transmission of fluorozirconate and fluorohafnate glasses. Xenon difluoride is a well-known fluoroxidizing agent for the fluorination of alkenes, acetylenes, aromatic and heteroaromatic molecules[11,12] and for the production of palladium fluorocomplexes[13] and layered copper oxofluorides.[14] Xenon difluoride was also effectively used for the removal of oxygen-containing impurities in the synthesis of potassium hexafluoromanganate.[15] XeF_2 is a colorless crystalline solid (T_m = 129 °C), making it an extremely easy-to-handle fluorinating agent. The only by-product of its reduction is elemental xenon.[16]

Glasses with the batch composition $58ZrF_4(HfF_4)\cdot 20BaF_2\cdot 2LaF_3\cdot 3AlF_3\cdot 17NaF$ were synthesized by melting stoichiometric amounts of starting fluorides at 900–950 °C in an argon atmosphere.

On the basies of the studied chemical transformations of RE, zirconium and hafnium oxides with the participation of xenon difluoride, the conditions for reactions (1)–(4) are determined, in which oxygen-free fluorides are formed.[17]

$$ZrO_2 + 2XeF_2 \xrightarrow{190\,^\circ\mathrm{C}} ZrF_4 + 2Xe + O_2, \tag{1}$$

$$HfO_2 + 2XeF_2 \xrightarrow{200\,^\circ\mathrm{C}} HfF_4 + 2Xe + O_2. \tag{2}$$

Fluorination of RE oxides proceeds in stages, with the formation of oxofluorides as the intermediate products, as follows:

$$La_2O_3 + XeF_2 \xrightarrow{350\,^\circ\mathrm{C}} 2LaOF + Xe + 0.5O_2, \tag{3}$$

$$LaOF + XeF_2 \xrightarrow{350\,^\circ\mathrm{C}} LaF_3 + Xe + 0.5O_2. \tag{4}$$

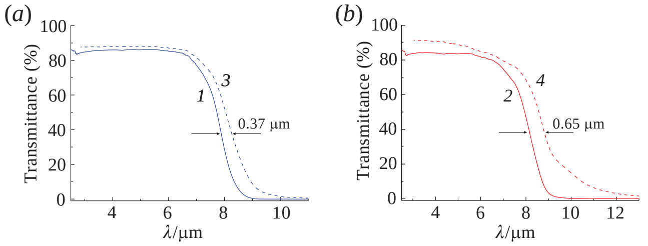

Figure 1 IR transmission spectra of (*a*) fluorozirconate and (*b*) fluorohafnate glasses: (*1*), (*2*) untreated and (*3*), (*4*) pre-treated with XeF_2. Numbering and glass compositions are listed in Table 1.

To treat the batch with xenon difluoride, the mixture of the initial fluorides and XeF_2 crystals was placed into a nickel autoclave lined with leucosapphire and connected to a vacuum line, and heated at 350 °C for 1.5 h. The excess of unreacted xenon difluoride and the evolved gaseous products were removed in a dynamic vacuum at 100 °C in order to prevent contamination of the synthesized glasses with bubbles and optical quality degradation.

Figure 1(*a*),(*b*) shows the IR transmission spectra[†] of glasses untreated and pre-treated with XeF_2. As seen from the figures, the treatment of the batch with xenon difluoride leads to the disappearance of the absorption band of the hydroxyl group in the region of 2.8 μm.

Calculation of the absorption coefficient α (Figure 2) shows that the fluorination of the batch leads to a lowering of the OH^- group content by almost an order.

In addition to the removal of the OH^- group absorption band, the treatment of the batch with xenon difluoride leads to a broadening of the transmission region of the glasses both in the UV and IR ranges. Figures 1 and 3 show the IR and UV transmission[‡] edges of fluorozirconate and fluorohafnate glasses without treatment and with treatment with XeF_2 (according to the level of 50% transmission).

In the hafnate glass, the IR transmission edge is shifted to the longer wavelength compared to the zirconate glass owing to the lower frequency vibrations of the Hf–F valence bonds than the Zr–F bonds, due to a larger hafnium atomic mass. The shift of the IR transmission edge to the longer wavelength in samples pre-treated with XeF_2 is associated with the removal of oxygen-containing impurities. The removal of oxygen leads the substitution of the metal–oxygen bonds with the lower-frequency metal–fluorine bonds.

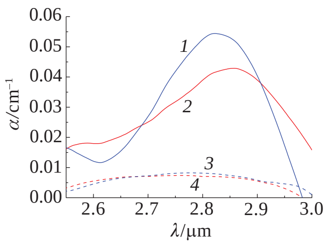

Figure 2 Absorption spectra of fluorozirconate and fluorohafnate glasses: (*1*), (*2*) untreated and (*3*), (*4*) pre-treated with XeF_2.

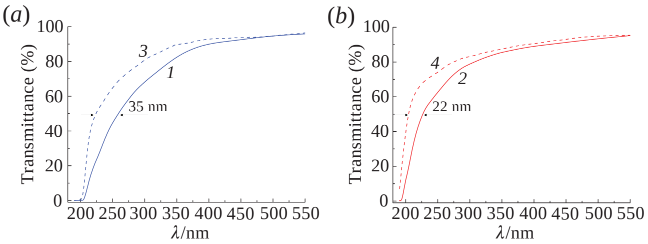

Figure 3 UV transmission spectra of (*a*) fluorozirconate and (*b*) fluorohafnate glasses: (*1*), (*2*) untreated and (*3*), (*4*) pre-treated with XeF_2. Numbering and glass compositions are listed in Table 1.

The UV transmission edge is determined by the electronic transitions from the valence band to the conduction band, *i.e.* band gap. The UV transmission edge of the fluorohafnate glass is shifted to the shorter wavelength relative to the fluorozirconate glass. It is conditioned by a larger band gap (ΔE) for the fluorohafnate glass, due to a higher ionicity of the $Hf^{4+}–F^-$ bond compared to $Zr^{4+}–F^-$, owing to the lower ionization potentials for hafnium (6.78–33.3 eV) than those for zirconium (6.84 –34.3 eV).[18] There are many local energy levels associated with the disordering of the structure (the so-called band tails) above the top of the valence band and below the bottom of the conduction band in the glass band gap. The levels are filled with electrons depending on the redox conditions for glass synthesis or treatment. The boundary between the filled and empty levels (the Fermi level, E_F) corresponds to the chemical potential of the glass. Oxidizing conditions cause depletion of levels, *i.e.* lowering the Fermi level. The actual transmission edge is determined by transitions from the upper filled local levels. When the glass is not treated with XeF_2, a significant part of the levels located above the valence band is filled with electrons, for example, up to the $E_{F'}$ level (Figure 4).

The electronic transitions from these levels determine the position of the UV transmission edge in the untreated glass. XeF_2 treatment partially empties the levels near the valence band to the E_F level, since fluorine, as a strong oxidizing agent, takes electrons from these levels, which leads to the disappearance of the corresponding transitions. As a result, the UV transmission edge is shifted to the shorter wavelength, since its position is now determined by the levels located closer to the valence band. Removal of oxygen also reduces absorption near the UV edge, since oxygen, which has a lower electron affinity (1.46 eV)[19] than fluorine (3.40 eV),[20] forms local levels above the valence band, and longer wavelength absorption corresponds to transitions from these levels (Figure 4). The obtained results are presented in Table 1.

In conclusion, pre-treatment of the initial fluorides with xenon difluoride results in a broadening of the transmission region in the fluorozirconate glass by 0.035 μm in the UV range [Figure 3(*a*)] and by 0.37 μm in the IR range [Figure 1(*a*)]. In the fluorohafnate glass the transmission region is broadened in the UV range up to 0.022 μm [Figure 3(*b*)], and in the IR range up to 0.65 μm [Figure 1(*b*)].

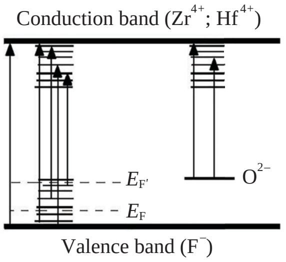

Figure 4 Band scheme of the fluoride glass.

[†] IR spectra of samples were recorded in the range of 4000–400 cm^{-1} on a Nicolet NEXUS IR-Fourier spectrometer (single-beam, scanning, beam splitter with a CsI coating, TGS detector with a CsI window, photometric accuracy 0.1%, resolution 2 cm^{-1}).

[‡] Transmission spectra in the UV–visible/NIR regions were measured on a JASCO V-770 spectrophotometer (JASCO Corporation, Japan) with a measurement range of 190–2700 nm at room temperature. For this, a pair of diffraction gratings is implemented: 1200 lines mm^{-1} (UV/Vis) and 300 lines mm^{-1} (NIR) and two automatically interchangeable detectors are provided: PMT (UV/Vis) and PbS (NIR) with Peltier cooling.

Table 1 Glass composition and optical properties.

No.	Glass composition/mol%	Absorption coefficient at λ = 2.8 μm/cm^{-1}	UV transmission edge/μm (eV)	IR transmission edge/μm (eV)
	Untreated glass			
1	$58ZrF_4{\cdot}20BaF_2{\cdot}2LaF_3{\cdot}3AlF_3{\cdot}17NaF$	0.054	0.256 (4.84)	7 (0.177)
2	$58HfF_4{\cdot}20BaF_2{\cdot}2LaF_3{\cdot}3AlF_3{\cdot}17NaF$	0.042	0.225 (5.51)	7.65 (0.162)
	Glass pre-treated with XeF_2			
3	$58ZrF_4{\cdot}20BaF_2{\cdot}2LaF_3{\cdot}3AlF_3{\cdot}17NaF$	0.008	0.221 (5.61)	7.5 (0.165)
4	$58HfF_4{\cdot}20BaF_2{\cdot}2LaF_3{\cdot}3AlF_3{\cdot}17NaF$	0.007	0.203 (6.11)	8.3 (0.149)

This research was funded by the Russian Science Foundation (RSF), grant no. 23-23-00586.

References

1 M. Poulain, S. Cozic and J. L. Adam, in *Mid-Infrared Fiber Photonics: Glass Materials, Fiber Fabrication and Processing, Laser and Nonlinear Sources*, eds. S. Jackson, M. Bernier and R. Vallée, Woodhead Publishing, 2022, pp. 47–109.

2 V. V. Sakharov, P. B. Baskov, O. V. Akimova, V. Sh. Berikashvili and G. F. Lebedev, *Inorg. Mater.*, 2008, **44**, 1386 (*Neorg. Mater.*, 2008, **44**, 1530).

3 B. Boulard, in *Functionalized Inorganic Fluorides: Synthesis, Characterization and Properties of Nanostructured Solids*, ed. A. Tressaud, Wiley, 2010, pp. 331–346.

4 M. G. Drexhage and C. T. Moynihan, *Sci. Am.*, 1988, **259**, 110.

5 N. T. Hung, N. T. Thuy, L. B. Thuan, D. T. T. Tra, D. Van Khoai, J. H. Jeon, J.-Y. Lee and R. K. Jyothi, *Mater. Today Chem.*, 2021, **22**, 100608.

6 A. Mukherjee and A. Awasthi, in *Thorium – Energy for the Future*, eds. A. Nayak and B. Sehgal, Springer, Singapore, 2019, pp. 225–232.

7 J. S. Sanghera, P. Hart, M. G. Sachon, K. J. Ewing and I. Aggarwal, *J. Am. Ceram. Soc.*, 1990, **73**, 1339.

8 M. Robinson, *Mater. Sci. Forum*, 1985, **5**–**6**, 19.

9 M. Brekhovskikh, V. Sukhoverkhov, V. Fedorov, S. Batygov, L. Dmitruk and N. Vinogradova, *J. Non-Cryst. Solids*, 2000, **277**, 68.

10 M. Brekhovskikh and V. Fedorov, *Extended Abstracts of the 10th International Symposium on Non-Oxide Glasses*, Corning, NY, USA, 1996, pp. 525–531.

11 B. Zajc and M. Zupan, *J. Org. Chem.*, 1982, **47**, 573.

12 G. Firnau, R. Chirakal, S. Sood and S. Garnett, *Can. J. Chem.*, 1980, **58**, 1449.

13 A. W. Kaspi, A. Yahav-Levi, I. Goldberg and A. Vigalok, *Inorg. Chem.*, 2008, **47**, 5.

14 A. M. Abakumov, M. G. Rozova, E. I. Ardashnikova and E. V. Antipov, *Russ. Chem. Rev.*, 2002, **71**, 383 (*Usp. Khim.*, 2002, **71**, 442).

15 M. N. Brekhovskikh, S. Kh. Batygov, L. V. Moiseeva, M. V. Mastryukov and K. S. Nikonov, *Mendeleev Commun.*, 2021, **31**, 887.

16 M. A. Tius, *Tetrahedron*, 1995, **51**, 6605.

17 M. N. Brechovskich, A. I. Popov, V. A. Fedorov and Yu. M. Kiselev, *Mater. Res. Bull.*, 1988, **23**, 1417.

18 A. V. Shevel’kov, A. A. Drozdov and M. E. Tamm, *Neorganicheskaya khimiya (Inorganic Chemistry)*, Laboratoriya znanii, Moscow, 2021 (in Russian).

19 M. K. Kristiansson, K. Chartkunchand, G. Eklund, O. M. Hole, E. K. Anderson, N. de Ruette, M. Kamińska, N. Punnakayathil, J. E. Navarro-Navarrete, S. Sigurdsson, J. Grumer, A. Simonsson, M. Björkhage, S. Rosén, P. Reinhed, M. Blom, A. Källberg, J. D. Alexander, H. Cederquist, H. Zettergren, H. T. Schmidt and D. Hanstorp, *Nat. Commun.*, 2022, **13**, 5906.

20 C. Blondel, C. Delsart and F. Goldfarb, *J. Phys. B: At. Mol. Opt. Phys.*, 2001, **34**, L281.

Received: 24th March 2023; Com. 23/7129